DOE/ARC-02-003

CONTINUING STUDIES ON DIRECT AQUEOUS MINERAL CARBONATION FOR CO_2 SEQUESTRATION

March 4-7, 2002

27th International Technical Conf. On Coal Utilization & Fuel Systems, Clear Water, FL

by W.K. O'Connor, D.C. Dahlin, D.N. Nilsen, S.J. Gerdemann, G.E. Rush, L.R. Penner, R.P. Walters, and P.C. Turner
Albany Research Center
Albany, Oregon

CONTINUING STUDIES ON DIRECT AQUEOUS MINERAL CARBONATION FOR CO_2 SEQUESTRATION

W.K. O'Connor, D.C. Dahlin, D.N. Nilsen, S.J. Gerdemann
G.E. Rush, L.R. Penner, R.P. Walters, and P.C. Turner

Albany Research Center
Office of Fossil Energy, USDOE
1450 Queen Ave SW
Albany, OR 97321

ABSTRACT

Direct aqueous mineral carbonation has been investigated as a process to convert gaseous CO_2 into a geologically stable, solid final form. The process utilizes a solution of sodium bicarbonate ($NaHCO_3$), sodium chloride (NaCl), and water, mixed with a mineral reactant, such as olivine (Mg_2SiO_4) or serpentine [$Mg_3Si_2O_5(OH)_4$]. Carbon dioxide is dissolved into this slurry, by diffusion through the surface and gas dispersion within the aqueous phase. The process includes dissolution of the mineral and precipitation of the magnesium carbonate mineral magnesite ($MgCO_3$) in a single unit operation. Activation of the silicate minerals has been achieved by thermal and mechanical means, resulting in up to 80% stoichiometric conversion of the silicate to the carbonate within 30 minutes. Heat treatment of the serpentine, or attrition grinding of the olivine and/or serpentine, appear to activate the minerals by the generation of a non-crystalline phase. Successful conversion to the carbonate has been demonstrated at ambient temperature and relatively low (10 atm) partial pressure of CO_2 (P_{CO2}). However, optimum results have been achieved using the bicarbonate-bearing solution, and high P_{CO2}. Specific conditions include: 185°C; P_{CO2}=150 atm; 30% solids. Studies suggest that the mineral dissolution rate is not solely surface controlled, while the carbonate precipitation rate is primarily dependent on the bicarbonate concentration of the slurry. Current and future activities include further examination of the reaction pathways and pretreatment options, the development of a continuous flow reactor, and an evaluation of the economic feasibility of the process.

INTRODUCTION

Concerns regarding the increasing concentrations of the "greenhouse gases," including carbon dioxide (CO_2), methane (CH_4), and water vapor, in the earth's atmosphere have led to calls for the reduction of CO_2 emissions from fossil-fuel-fired power plants. In response, the U.S. Department of Energy (DOE) Office of Fossil Energy has identified the mitigation of the effects of CO_2 emissions as a critical research issue for its Vision XXI power plant. Sequestration of CO_2 by several potential methods is under investigation as a means to limit CO_2 emissions into the atmosphere, including terrestrial and ocean sequestration, geological sequestration, and advanced concepts, such as mineral carbonation.

The basis for the aqueous carbonation reaction is the natural alteration of ultramafic rocks, such as peridotites, pyroxenites, and dunites (>90% olivine), called serpentinization. These rocks

contain high concentrations of magnesium, and when formation waters contact the ultramafic sequence, usually under high pressure at moderate temperatures, alteration to the hydrated magnesium silicate, serpentine, occurs. When these waters contain dissolved CO_2, magnesite may form as a secondary alteration mineral.

The serpentinization reaction occurs in nature, and is favored thermodynamically, although the natural reaction rate is slow. Increased partial pressure of CO_2 (P_{CO2}), concentration of CO_2 in solution, reaction catalysis, thermal or mechanical activation, or some combination of these, could increase the reaction rate dramatically. Optimization of these parameters will determine the feasibility of the aqueous carbonation reaction as a viable CO_2 sequestration option.

TECHNICAL PROGRESS

Initial research studies consisted primarily of proof-of-concept experiments to confirm the carbonation reaction of natural olivine; equation (1).

$$\underset{\text{Olivine}}{Mg_2SiO_4} + \underset{\text{Carbon dioxide}}{2CO_2} \xrightarrow{298K} \underset{\text{Magnesite}}{2MgCO_3} + \underset{\text{Silica}}{SiO_2} + 54\ kJ \qquad \text{Eq. 1}$$

Bench-scale tests were begun with 5-gram samples of sized foundry-grade olivine sand, distilled water, and cylinder CO_2 in a 45-ml autoclave. Ambient and elevated temperature (22° and 150°C) and elevated pressure (30 and 50 atm) were evaluated in long-duration tests. No discernible reaction took place at low temperature and pressure, but over 80 pct stoichiometric conversion to carbonate was achieved at 150°C and 50 atm after 144 hours. Magnesite was confirmed by X-ray diffraction (XRD).

Over the next 3 years, improvements to the experimental apparatus, modifications to the carbonation solution, and pretreatment of the mineral reactants resulted in dramatic increases in reaction rate and conversion efficiency. Studies were expanded to include the carbonation of additional mineral reactants, primarily serpentine; equation (2).

$$\underset{\text{Serpentine}}{Mg_3Si_2O_5(OH)_4} + \underset{\text{Carbon dioxide}}{3CO_2} = \underset{\text{Magnesite}}{3MgCO_3} + \underset{\text{Silica}}{2SiO_2} + \underset{\text{Water}}{2H_2O} \qquad \text{Eq. 2}$$

Over 300 batch experiments, at the 100-300 gram scale, were conducted in a continuously-stirred 2-liter autoclave coupled to a CO_2 gas booster pump. Improvements made to the process and specific accomplishments are summarized below, with a timeline included in Figure 1.

1. Investigated test parameters above the critical point of CO_2 (31°C and 72.9 atm), up to 250°C at P_{CO2} = 150 atm, reduced reaction time (to achieve ~80 pct stoichiometric conversion to the carbonate) to 24 hours (*1*);
2. Modified solution chemistry to include 0.64 M $NaHCO_3$, 1 M NaCl, reduced reaction time from 24 to 6 hours (*2*);

3. Identified heat treatment as an effective activation method for serpentine minerals at an optimum temperature range of 615-630°C (energy demand ~250 kW•h/ton) (*3*);
4. *Demonstrated ~75 pct stoichiometric conversion of heat activated antigorite to magnesite in 30 minutes, at 155 °C, P_{CO2} = 150 atm*;
5. Conducted pilot-scale comminution tests on the mineral reactants, including an effective magnetic separation step to produce an iron oxide by-product, determined a Grinding Index of 11.5 kW•h/ton to minus 200 mesh (75 microns) (*4*);
6. Identified mechanical activation, by high intensity attrition grinding to minus 10 microns, as an effective activation method for olivine, *achieved >80 pct stoichiometric conversion of attritted olivine to magnesite in less than 1 hour at 185 °C, P_{CO2} = 150 atm*;
7. Identified mechanical activation (attrition grinding) as an effective alternative to thermal activation for serpentine, and the *potential for ambient temperature, low P_{CO2} (10 atm) carbonation of mechanically activated mineral reactants* (*5*).

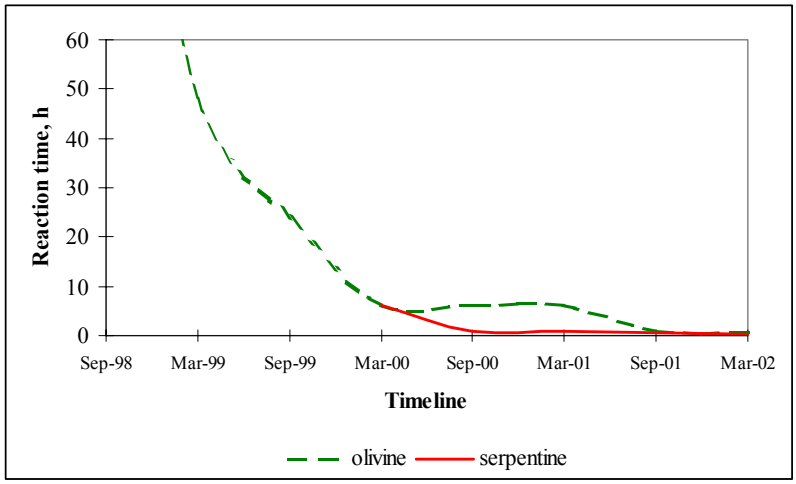

Figure 1.- Timeline for reduction of olivine and serpentine carbonation reaction times (to ~80% conversion).

Current research is concentrated on the mechanisms for mineral activation, by either thermal or mechanical processes, and further interpretation of the reaction sequence. The dramatic increase in mineral reactivity achieved by attrition grinding has made low temperature and pressure (T=20°C, P_{CO2}=10 atm) carbonation possible. The low temperature carbonation changed the character of the carbonate mineral product and provided insight into the complicated reaction process. Discussion of these two areas of focus is included in the main body of the paper.

MATERIALS

Mineral Availability

An evaluation of serpentine and olivine resources is not complete, but the pertinent literature suggests that serpentine resources far surpass the possible demand, while olivine resources, though tremendous in volume, are more limited. For example, the Twin Sisters Deposit in northwest Washington state is estimated to contain over 2 billion tons of unaltered dunite, a rock composed of greater than 90% olivine (*6*). Assuming 100% ore recovery, a 2:1 ore to CO_2 ratio, and ~80% carbonation efficiency, this is sufficient olivine to carbonate 100% of the CO_2 emissions from 8-10 1 GW coal-fired power plants for ~15 years. While this represents a tremendous resource of olivine, its use would likely be limited to the northwestern U.S. and southwestern Canada. Long-range transportation of the ore would be impractical.

Commercially exploited deposits of olivine are found around the world, with the most notable occurring in Mexico, Austria, Italy, Norway, the USA, Spain, Japan, and Pakistan (*7*). A survey of olivine deposits in the southeastern U.S. was conducted by Hunter (*8*).

While high grade olivine, or dunite, generally occurs in concentrated deposits with limited extent, serpentine occurs in massive ultramafic sequences, or ophiolite belts, generally located along continental margins or suture zones (*9*). These ophiolites were formed by convergent tectonic forces, and represent the remnants of ancient seafloors. Massive occurrences are found along both coasts of North America, and in South America (Brazil), northern Europe, west Africa, Asia Minor, the Arabian peninsula, central Asia, India, Indonesia, Japan, and Australia. Goff, et al, has conducted a survey of ultramafic deposits in the U.S. with respect to carbonation potential (*10,11*).

Mineral Chemistry

Olivine and serpentine actually represent two distinct mineral groups. Olivine includes the solid solution series between magnesium-rich (forsterite) and iron-rich (fayalite) end members. Forsterite is by the far the most abundant olivine mineral in nature, though some Fe in substitution for Mg is always present. For simplicity in this document, olivine and forsterite are used interchangeably. Serpentine refers to a group of three minerals, antigorite, lizardite, and chrysotile (asbestos). Serpentine occurrences tend to be dominated by either of the first two minerals, with chrysotile as a minor constituent. The subject studies have included three magnesium silicate minerals, olivine, antigorite, and lizardite.

Head analyses of the mineral reactants consistently show Mg concentrations in the olivine, antigorite, and lizardite of ~30, 26, and 24 wt pct, respectively. The lower Mg concentration in the serpentine minerals is due to the presence of ~14 wt pct chemically-bound water. The carbonation potential of the head materials can be calculated based on their Mg concentration and the stoichiometry of equations 1 and 2. This potential can be quantified gravimetrically as the ratio – weight of CO_2 carbonated:weight of mineral reactant, or 0.55, 0.48, and 0.45 for these samples of olivine, antigorite, and lizardite, respectively. Assuming 100% conversion of the silicate Mg to carbonate, the total weight of product solids, and percentage weight increase (ε_A) were also calculated. Extent of reaction (X_R) was determined by comparison of the actual CO_2 concentration (A) in the product solids, as determined by chemical analysis, to this 100% conversion value, equation 3. An example calculation follows.

Basis: 100 g olivine; 30 wt pct Mg; 100% carbonate conversion
MW of Mg_2SiO_4 = 140 g/g mol; Mg in Mg_2SiO_4 = 34.3%
MW of CO_2 = 44g/g mol

Weight of Mg = 30 g; 30 g/0.343 = 87.5 g (weight of Mg_2SiO_4); moles Mg_2SiO_4 = 0.625;
2 moles CO_2:mole Mg_2SiO_4 (eq. 1), moles CO_2 = 1.25; % weight gain (CO_2) = ε_A = 0.55;

$$X_R = \frac{A}{\varepsilon_A (100 - A)} \qquad \text{Eq. 3}$$

EXPERIMENTAL RESULTS

Mineral Activation

Activation of the mineral reactants has been achieved by both thermal and mechanical means, although the mechanism for this activation was not clearly understood. Some discussion of the enhancement of Mg silicate solubility by mechanical means is included in prior literature (*12*). Because most mineral dissolution reactions are surface controlled, it was possible that the two pretreatment methods proved successful due to increased surface area. Under this scenario, mechanical pretreatment further reduced the mean particle size of the minerals, while thermal pretreatment removed chemically-bound water, which may have increased the porosity and the resulting surface area. However, studies conducted at Arizona State University, a collaborating laboratory with ARC, suggested that the activation was due to destruction or disordering of the crystalline nature of the minerals (*13*). To better identify the activation mechanism(s), characterization studies including particle size, surface area, porosimetry, and X-ray diffraction (XRD) analysis were conducted on the each of the materials.

Particle Analysis

The olivine, antigorite, and lizardite head materials were ground through 200 mesh (75 μm) to provide a stockpile of baseline material for all subsequent testing. Particle size analysis by Micromeretics Sedigraph, nitrogen adsorption BET surface area, and porosimetry analyses were conducted on these head materials and their respective pretreatment products. The relevant statistical data are included in Table 1, while the cumulative mass percent finer vs. particle diameter curves are included in Figures 2-4.

Table 1.- Relevant particle size analysis, surface area, and porosimetry for the mineral reactants.

	Particle Diameter (μm) Mass Distribution Arithmetic Statistics								
	-75 μm heads			Heat treated		Attritted olivine (1 h)		Attritted (1 h, dry)	
Measurement	olivine	antigorite	lizardite	antigorite	lizardite	dry	wet	antigorite	lizardite
Mean	25.85	23.81	26.62	25.72	28.57	10.15	5.228	7.683	8.831
Mode	35.48	39.81	37.58	42.17	33.5	4.217	3.981	9.441	12.59
Median (D50)	19.46	13.36	19.08	16.81	22.11	4.335	1.915	4.172	4.984
	Nitrogen Adsorption Statistics								
BET SA[1]	4.600	8.509	32.288	18.680	10.842	5.092	46.293	28.615	33.763
Pore volume[2]	0.0118	0.0404	0.0647	0.0668	0.0516	0.0375	0.1213	0.1296	0.1481
Pore diameter[3]	102.587	189.770	80.155	142.927	190.541	294.474	104.748	181.173	175.506

[1] BET surface area, m^2/g.

[2] Total pore volume of pores less than 2494 A diameter at P/P_o 0.9922.

[3] Average pore diameter, Angstroms.

Mean particle diameters for all three head materials are very uniform, while attrition grinding significantly reduced the mean particle diameters and overall size distributions. This size reduction was particularly dramatic for the wet attritted olivine product, which had a mean particle diameter roughly half that of the dry attritted olivine. The BET surface area measurements showed an even greater disparity between the two attrition methods. Dry attrition grinding did not result in an increase in the relative surface area, while the surface area of the wet attritted product increased by an order of magnitude over that of the head. Wet grinding is considered more efficient than dry, but the difference between these two materials cannot be

explained by conventional grinding efficiencies. A more likely explanation is a phenomenon known as “cold bonding” that is known to occur when attritioning metal powders. The grinding energy in an attrition mill is so intense that micron-sized particles re-agglomerate into larger aggregates. The attritted material thus exhibits the physical properties of coarser materials. Wet attrition grinding may prevent this re-agglomeration by limiting heat generation at the particle surface. The average pore diameter measurements tend to support this assertion. The mean pore diameter of the olivine head and wet attritted product were virtually identical, at just over 100 Angstroms. This would be expected when simple particle size reduction takes place. The dramatic rise in surface area would also be expected. However, the mean pore diameter of the dry attritted olivine was nearly 3 times that of the other two olivine materials. Agglomerates of much finer particles could produce the relatively large pore diameter while limiting surface area.

Lizardite behaved very similarly to olivine with respect to dry attrition grinding. Surface area remained nearly constant while the mean pore diameter increased significantly, again exhibiting attributes of an aggregate of much finer particles.

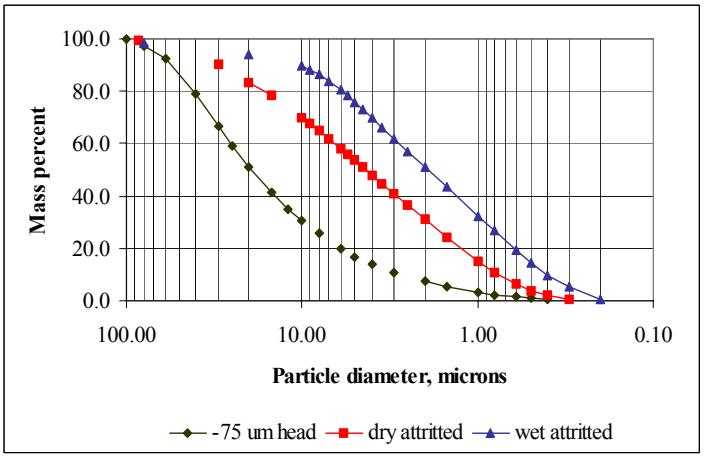

Figure 2.- Cumulative mass percent vs. diameter for the olivine materials.

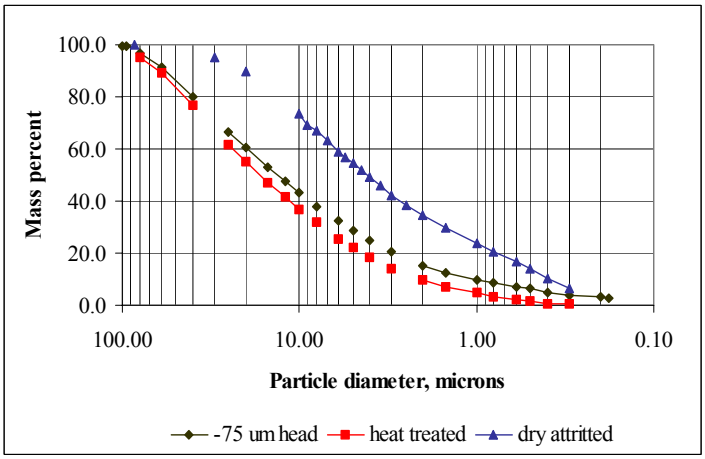

Figure 3.- Cumulative mass percent vs. diameter for the antigorite materials.

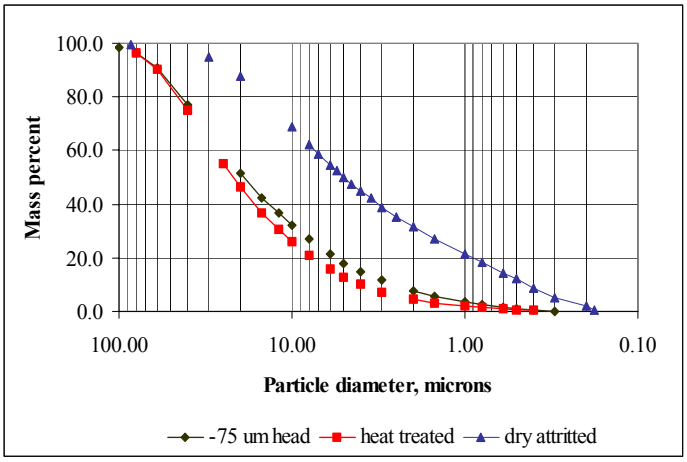

Figure 4.- Cumulative mass percent vs. diameter for the lizardite materials.

However, the surface area and mean pore diameter of the attritted antigorite exhibit just the opposite (increased surface area with no change in pore diameter). At the heart of this disparate behavior may be the differing atomic structures of the two serpentine minerals, which include a brucite [$Mg(OH)_2$] type layer fitted to a tetrahedral Si_2O_5 sheet (*14*). The imperfect fit between these layers is compensated for by a bending of the tetrahedral layer. In antigorite, the bending is not continuous but occurs as corrugations. Lizardite may have a structure more analogous to chrysotile, in which the bending is continuous. Although heat treatment does not result in further size reduction of either serpentine mineral, the relative surface area of antigorite increases while that of lizardite decreases. This may indicate that dehydroxylation of the lizardite causes a collapse of its structure, while the antigorite structure is more resistant to collapse, thus dehydroxylation increases porosity and relative surface area. Definitive resolution of these peculiar phenomena is left to future studies. Most critical at this time is correlating the particle analysis data with the performance of these materials in the mineral carbonation reaction.

Reaction Kinetics

Simplified reaction rates were determined for each of the mineral heads and pretreatment products described above. These rates refer to mass conversion of Mg silicate to Mg carbonate, and are not to be confused with rate constants. Total mass of Mg in the feed multiplied by the extent of reaction (X_R) was divided by the reaction time, resulting in a reaction (conversion) rate in grams of Mg converted to the carbonate per hour of reaction time. To compensate for variations in surface area, it was added to the conversion rate equation, resulting in a normalized conversion rate (R_X) in grams of Mg converted to the carbonate per m^2 of surface area per hour of reaction time. The conversion rate data are included in Table 2.

Table 2.- Conversion data for the mineral carbonation reaction, normalized to surface area.

Test[1] no.	Feed material	Mg wt pct	Mg wt, g	Reaction time, h	X_R[2] pct stoich.	Surface area m^2/g	Total surface area, m^2	R_X[3] g $Mg/m^2/h$
SC-234	-75 μm olivine	29.8	49.8	3.0	36	4.6	768.1	0.008
SC-151	-75 μm antigorite	23.1	38.6	1.0	14	8.5	1421.0	0.004
SC-154	-75 μm lizardite	23.7	39.6	1.0	4	32.3	5392.0	0.0003
SC-145	HT[4] -75 μm antigorite	30.2	50.4	1.0	49	18.7	3119.6	0.008
SC-163	HT[4] -75 μm lizardite	25.8	43.1	1.0	38	10.8	1810.6	0.009
SC-257	Attritted[5] olivine	28.1	46.9	1.0	76	5.1	850.3	0.042
SC-265	Attritted olivine (wet)	25.6	46.9	1.0	100	46.3	7730.9	0.006
SC-279	Attritted antigorite	24.6	41.1	1.0	46	28.6	4778.6	0.004
SC-283	Attritted lizardite	20.7	34.6	1.0	45	33.8	5638.4	0.003

[1] Carbonation tests conducted @ 15% solids: 167 grams solids in 946 grams 0.64 M $NaHCO_3$, 1 M NaCl solution.
[2] Extent of reaction, percent stoichiometric conversion of Mg silicate to Mg carbonate.
[3] Normalized conversion rate, grams of Mg carbonated per m^2 per hour of reaction time.
[4] HT: Heat treated @ 630°C for 1 hour, in air.
[5] Attrition tests were conducted dry, on the –75 μm head materials for 1 hour, unless otherwise noted.

The aqueous mineral carbonation process includes both silicate dissolution and carbonate precipitation reactions, thus the R_X cannot be isolated to either of the separate reactions.

However, experience with the process suggests that mineral dissolution is rate limiting, so greater rate of conversion is likely the result of increased mineral solubility.

The normalized conversion rates provide excellent insight into the effect of thermal and mechanical activation methods. Baseline conversion rates were calculated for each of the mineral reactants. These materials underwent no pretreatment other than size reduction to minus 200 mesh (75 μm). Olivine is clearly the most reactive mineral, at roughly double the normalized conversion rate (R_X) for antigorite and up to 30 times the rate for lizardite. Heat treatment of the serpentine minerals improved both R_X to the level of olivine, this despite the fact that lizardite surface area decreased with heat treatment. This strongly suggests that the mineral dissolution rate was not solely surface controlled, and some other phenomenon was responsible, such as the partial destruction or disordering of the mineral lattice.

Mechanical activation by attrition grinding was informative. Dry attrition grinding of the olivine produced >400% increase in R_X, without increasing the relative surface area, while the R_X for the wet attritted olivine actually dropped to ~50% of the rate measured for the olivine head. The fact that X_R for the wet attritted olivine (100%) exceeded that for both the dry attritted olivine (82%) and the olivine head (47%) suggests that the improved X_R was due exclusively to the dramatic increase in surface area for the wet attritted olivine. The larger mean particle diameter and lower surface area of the dry attritted olivine and olivine head, compared to the wet attritted olivine, may mean that the reaction is diffusion limited. Extremely fine grinding can overcome diffusion limitations. However, considering the much higher R_X for the dry attritted olivine, it is likely that shorter duration tests would result in a reversal in X_R between the two attrition products. This contention is supported by observations made during the carbonation tests. An exotherm was observed immediately upon pressurization of the reactor during the test conducted on the dry attritted olivine. This exotherm had not been observed during any previous test, including the wet attritted olivine test, and is attributed to the Mg carbonation reaction (eq. 1). This suggests that magnesite precipitation occurred simultaneously with silicate dissolution. It also suggests that low temperature and reduced P_{CO2} carbonation is possible. These observations were made on a material with relatively high mean particle diameter and low surface area, again pointing out that some phenomenon other than increased surface area was responsible for activation.

X-Ray Diffraction Studies

X-ray diffraction (XRD) analysis was conducted on all reactants to identify any alterations to the crystalline nature of the minerals imparted by the thermal and mechanical pretreatment methods. Dramatic changes in the diffraction patterns for some of the materials were correlated with the particle analysis and conversion rate data, providing a strong indication that destruction of the crystal lattice is a major factor in activation of the mineral reactants.

Diffraction patterns for the head, dry attritted, and wet attritted olivine materials are included in Figures 5-7. The diffractogram for the olivine head is a typical pattern for forsterite olivine. Intensities for the major peaks exceed 2,500 counts. In contrast, the dry attritted olivine shows significant reduction in peak intensities, with an increased background indicative of amorphous material. The diffractogram for the wet attritted olivine is again typical of forsterite, nearly

duplicating the pattern for the olivine head. These results compliment the particle analysis and conversion rate data, which suggested that activation of the wet attritted olivine was primarily due to size reduction and increased surface area. The XRD data indicate that activation of the dry attritted olivine was due to disruption of the crystal lattice.

Space does not permit the inclusion of the diffraction patterns for the antigorite materials, but they exhibit a similar trend. Peak intensities of the heat treated antigorite decrease significantly compared to the head, and peaks characteristic of forsterite begin to appear. This partial transformation to forsterite is expected, and parallels the conversion rate data which showed identical R_X for the heat treated antigorite and olivine head material. Attrition grinding had a much more dramatic effect on the XRD pattern, reducing peak intensities even further, suggesting a significant amount of amorphous material was present. However, R_X for the attritted antigorite was roughly half that for the heat treated antigorite, and was much lower than the R_X for the dry attritted olivine. Attrition grinding does not remove the chemically-bound water from the serpentine, and the presence of this water may explain the lower reactivity of the antigorite compared to the olivine. This suggests that combined thermal and mechanical pretreatment may be most effective for activation of the serpentine minerals.

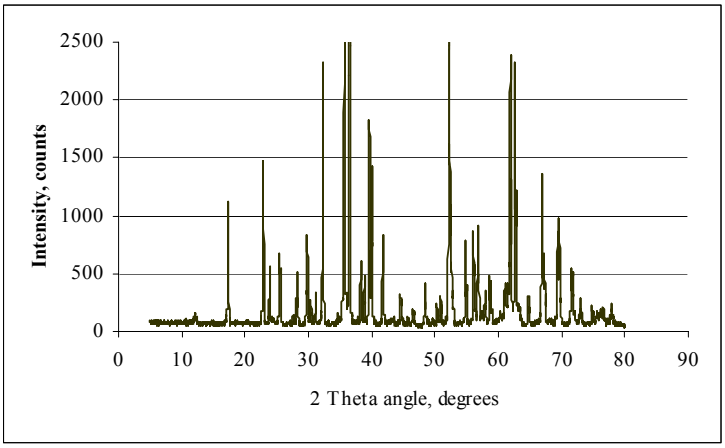

Figure 5.- XRD diffractogram of olivine head.

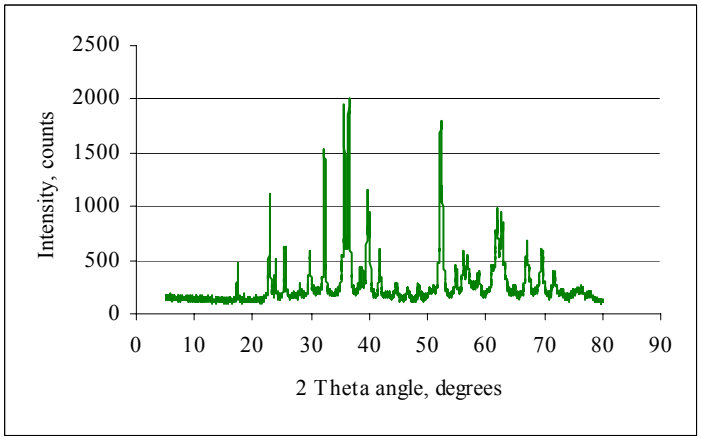

Figure 6.- XRD diffractogram of dry attritted olivine.

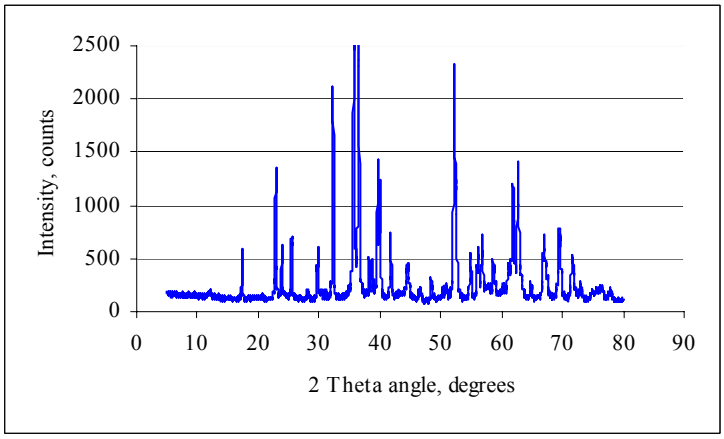

Figure 7.- XRD diffractogram of wet attritted olivine.

Reaction Sequence

Mg Solubility

In addition to studies on the conversion rate of the mineral carbonation reaction, efforts were made to clarify the actual reaction sequence. Analyses show that the particle size of the magnesite product is limited to –10 μm, which led to much speculation regarding the timing of magnesite precipitation. One explanation for the limited magnesite particle size was rapid, late-stage precipitation. However, this explanation would require high Mg solubility (~45 g/L) in the carbonate solution to account for tests with X_R >80%. Prior literature provides Mg solubility data that tend to refute the late-stage precipitation sequence (*15*). Curves for Mg solubility in water over an equilibrium temperature range of 5-60°C and P_{CO2} of 1-34 atm are included in Figure 8. Although these conditions do not match those used for the majority of the carbonation tests (155-185°C and P_{CO2} ~150 atm), the trends are relevant. Maximum Mg solubility occurs at low temperature and high P_{CO2}, making it unlikely that the Mg solubility at the high reaction temperatures used could reach 45 g/L. In addition, the increasing Mg solubility with decreasing temperature would discourage late-stage magnesite precipitation, and suggests that the product solutions should be high in Mg concentration. However, Mg concentration in the carbonation product solutions is only ~200 mg/L. These factors argue that magnesite precipitation had occurred prior to the late-stage cool-down of the autoclave reactor. Early-stage magnesite precipitation, simultaneous with Mg silicate dissolution, could also result in the limited particle size of the product. An inherent property of the precipitate, agitation within the continuously-stirred autoclave reactor, or some combination of the two could be at play. Prior literature reports similar size limitations for precipitated magnesite, and tends to support early-stage precipitation (*16,17*).

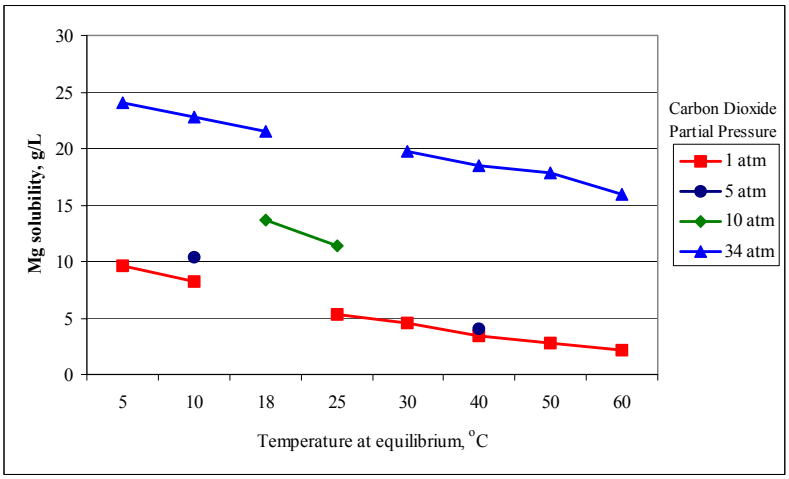

Figure 8.- Mg solubility vs. temperature at various P_{CO2} (after Linke, *15*).

Low Temperature Carbonation

The initial attrition grinding tests were conducted for extreme time frames up to 24 hours. These proof-of-concept tests were not applicable to an industrial process, but produced an extremely reactive mineral product that was found to carbonate at low temperature and P_{CO2}. These ambient temperature (20°C) tests, conducted at P_{CO2} = 10 atm, provided evidence that reaction conditions could be lowered dramatically with effective mineral pretreatment. The tests also produced a reaction exotherm and solid carbonate product that tend to corroborate the Mg solubility data, and support the premise that magnesite precipitation occurs as Mg is dissolved from the silicate mineral. This reaction exotherm is the first measurable evidence that early-stage carbonate precipitation occurs during the course of the reaction. The identification of hydromagnesite [$3MgCO_3.Mg(OH)_2.3H_2O$] in the reaction products from the ambient

temperature tests is further evidence in support of early-stage precipitation in the high temperature tests. Hydromagnesite is unstable at temperatures above ~100°C, but if the late-stage precipitation premise is correct, hydromagnesite should form as the reactor is cooled below 100°C. However, magnesite was the only Mg carbonate identified in the high temperature carbonation test products. The identification of hydromangestite by XRD, rather than magnesite, in the solid products from the ambient temperature tests suggests that hydromagnesite is the favored carbonate precipitate when carbonation occurs at temperatures well below 100°C. Figure 9 includes differential thermal analysis (DTA) and thermal gravimetric analysis (TGA) curves for the reaction products from low temperature carbonation tests with X_R ~80%. The curves show initial decomposition of the hydromagnesite at <100°C, a temperature well below the range used for high temperature (155-185°C) carbonation.

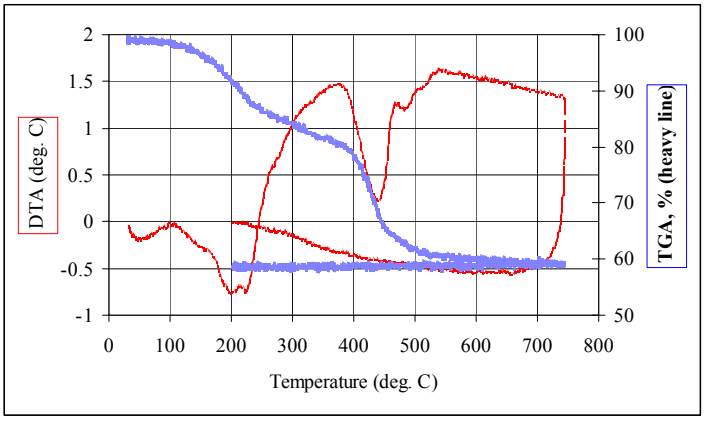

Figure 9.- DTA/TGA for low temperature carbonation product (hydromagnesite).

CONCLUSIONS

An aqueous mineral carbonation process has been developed over the past four years for the reaction of Mg silicate minerals with CO_2 to form Mg carbonates. Recently, improvements in extent of reaction (X_R) and rate of conversion (R_X) have led to an expansion of the research efforts to include a process feasibility study and the development of a continuous flow reactor. Significant conclusions made from the subject studies are summarized below.

1. Activation of the mineral reactants can be achieved by both thermal (serpentine minerals) and mechanical (olivine and serpentine minerals) methods.
2. Mineral activation follows two paths: (1) size reduction to increase relative surface area; and (2) destruction or disordering of the crystal lattice to form an amorphous material.
3. Olivine activation by mechanical means was achieved by both paths described in #2. Size reduction to increase relative surface area (wet attrition grinding) improves X_R, while destruction of the crystalline nature of the mineral (dry attrition grinding) improves R_X.
4. Serpentine activation by thermal treatment (1 hour at 630°C, in air) exceeded that achieved by mechanical treatment (1 hour dry attrition grinding). Because mechanical activation does not result in dehydoxylation of the serpentine (as does thermal activation), a combined thermo-mechanical activation methodology may prove most effective.
5. The aqueous mineral carbonation reaction sequen`ce includes early-stage precipitation of Mg carbonate, simultaneous with silicate dissolution.

REFERENCES

1. O'Connor, W.K., Dahlin, D.C., Turner, P.C., and Walters, R.P., "Carbon Dioxide Sequestration by Ex-Situ Mineral Carbonation," *Technology*, Vol. 7S, pp. 115-123.
2. O'Connor, W.K., Dahlin, D.C., Nilsen, D.N., Rush, G.E., Turner, P.C., and Walters, R.P., "CO_2 Storage in Solid Form: A Study of Direct Mineral Carbonation," *Proc. of the 5th Inter. Conference on Greenhouse Gas Technologies,* Cairns, Australia, August 14-18, 2000, 7 pp.
3. Dahlin, D.C., O'Connor, W. K., Nilsen, D.N., Rush, G.E., Walters, R.P., and Turner, P.C., "A Method for Permanent CO_2 Sequestration: Supercritical CO_2 Mineral Carbonation," *Proc. of the 17th Annual Inter. Pittsburgh Coal Conf.*, Pittsburgh, PA, Sept. 11-15, 2000, 14 pp.
4. O'Connor, W. K., Dahlin, D.C., Rush, G.E., Dahlin, C.L., and Collins, W.K., "Carbon Dioxide Sequestration by Direct Mineral Carbonation: Process Mineralogy of Feed and Products," *Preprint No. 01-9, SME Annual Meeting,* Denver, CO, Feb. 26-28, 2001, 9 pp.
5. O'Connor, W.K., Dahlin, D.C., Nilsen, D.N., Gerdemann, S.J., Rush, G.E., Walters, R.P., and Turner, P.C., "Research Status on the Sequestration of Carbon Dioxide by Direct Aqueous Mineral Carbonation," *Proc. of the 18th Annual Inter. Pittsburgh Coal Conference, Session 35, Paper 35-1*, Newcastle, NSW, Australia, December 3-7, 2001, 11 pp.
6. Smith, C. Jr., "Olivine the Industrial Mineral," *Preprint No. 92-102, SME Annual Meeting,* Phoenix, AZ, February 24-27, 1992, 4 pp.
7. Skillen, A, "Olivine: Long Live the Evolution," *Industrial Minerals*, Feb. 1995, pp 23-31.
8. Hunter, C. E. "Forsterite Olivine Deposits of North Carolina and Georgia." Raleigh, NC: *North Carolina Department of Conservation and Development; Bulletin 41*; 1941, 117 pp.
9. IGCP (International Geological Program). North American Ophiolites. Coleman, R. G., and Irwin, W. P., eds. "Ophiolites of continents and comparable oceanic rocks." Portland, OR: *State of Oregon, Dept. of Geol. and Min. Ind.; Bulletin 95*; 1977, 183 pp.
10. Goff, F., Guthrie, G., Counce, D., Kluk, E., Bergfeld, D., and Snow, M., "Preliminary Investigations on the Carbon Dioxide Sequestering Potential of Ultramafic Rocks," Los Alamos, NM, Los Alamos National Laboratory, LA-13328-MS, 1997.
11. Goff, F., Guthrie, G., Lipim, B., Chipera, S., Counce, D., Kluk, E., and Ziock, H., "Evaluation of Ultramafic Deposits in the Eastern United States and Puerto Rico as Sources of Magnesium for Carbon Dioxide Sequestration," Los Alamos, NM, Los Alamos National Laboratory, LA-13694-MS, 2000, 36 pp.
12. Zhang, Q., Sugiyama, K., and Saito, F., "Enhancement of Acid Extraction of Magnesium and Silicon from Serpentine by Mechanochemical Treatment." *Hydrometallurgy*, **45**, pp. 323-331, 1996.
13. McKelvy, M.J., Chizmeshya, A.V.G., Bearat, H., Sharma, R., and Carpenter, R.W., "Developing Mechanistic Understanding of CO_2 Mineral Sequestration Reaction Processes," *Proc. Of the 26th International Tech. Conference on Coal Utilization & Fuel Systems, pp. 777-788*, Clearwater, Florida, March 5-8, 2001.
14. Hurlbut, C.S. Jr., and Klein, C, "*Manual of Mineralogy (After J.D. Dana)*," 19th Ed., John Wiley & Sons, New York, New York, 1977.
15. Linke, William F., "*Solubilities of Inorganic and Metal-Organic Compounds*," Vol. 2, Fourth Ed., American Chemical Society, Washington D.C., 1965.
16. Ityokumbul, M.T., Chander, S., O'Connor, W.K., Dahlin, D.C., and Gerdemann, S.J., "Reactor Design Considerations in Mineral Sequestration of Carbon Dioxide," *Proc. of the 18th Annual Inter. Pittsburgh Coal Conference, Session 17, Paper 17-4*, Newcastle, NSW, Australia, December 3-7, 2001, 9 pp.
17. Devasahayam, S., and Khangoankar, P.R., "Particle Characteristics of Precipitated Magnesium Carbonate," *Minerals and Metallurgical Processing*, **12** (3), pp. 157-160, 1995.